Meiotic Telomere Protein Ndj1p Is Required for Meiosis-specific Telomere Distribution, Bouquet Formation and Efficient Homologue Pairing

Edgar Trelles-Sticken,* Michael E. Dresser,‡ and Harry Scherthan*§

*Department of Human Biology and Genetics, University of Kaiserslautern, D-67653 Kaiserslautern, Germany; ‡Program in Molecular and Cell Biology, Oklahoma Medical Research Foundation, Oklahoma City, Oklahoma 73104; and §Department of Cell Biology, University of Kaiserslautern, D-67653 Kaiserslautern, Germany

Abstract. We have investigated the requirements for *NDJ1* in meiotic telomere redistribution and clustering in synchronized cultures of *Saccharomyces cerevisiae*. On induction of wild-type meiosis, telomeres disperse from premeiotic aggregates over the nuclear periphery, and then cluster near the spindle pole body (bouquet arrangement) before dispersing again. In *ndj1Δ* meiocytes, telomeres are scattered throughout the nucleus and fail to form perinuclear meiosis-specific distribution patterns, suggesting that Ndj1p may function to tether meiotic telomeres to the nuclear periphery. Since *ndj1Δ* meiocytes fail to cluster their telomeres at any prophase stage, Ndj1p is the first protein shown to be required for bouquet formation in a synaptic organism. Analysis of homologue pairing by two-color fluores-

cence in situ hybridization with cosmid probes to regions on *III, IX,* and *XI* revealed that disruption of bouquet formation is associated with a significant delay (>2 h) of homologue pairing. An increased and persistent fraction of *ndj1Δ* meiocytes with Zip1p polycomplexes suggests that chromosome polarization is important for synapsis progression. Thus, our observations support the hypothesis that meiotic telomere clustering contributes to efficient homologue alignment and synaptic pairing. Under naturally occurring conditions, bouquet formation may allow for rapid sporulation and confer a selective advantage.

Key words: bouquet fluorescence in situ hybridization • *ndj1* • chromosome pairing • meiosis • telomeres

Introduction

The ends of eukaryotic chromosomes (telomeres) consist of simple DNA repeats associated with proteins and play important roles in replication, malignant transformation, and cellular aging (for reviews, see Blackburn, 1991; Zakian, 1995; de Lange, 1998a; Shore, 1998). Besides the vital functions telomeres perform in vegetative cells, they have been implicated as key players in the chromosome pairing process during meiosis (Moses, 1968; Loidl, 1990; Dernburg et al., 1995; Roeder, 1997; de Lange, 1998b; Zickler and Kleckner, 1998). The pairing of homologues and their recombination during meiotic prophase is critical for reduction of DNA content from diploid to haploid before fertilization (von Wettstein et al., 1984; Hawley, 1988). In many organisms, the premeiotic (vegetative) telomere distribution is altered during the onset of prophase I such that telomeres attach to the inner nuclear membrane, and then move along it to cluster in a limited nuclear envelope sector at the onset of zygotene (von Wettstein et al., 1984). This bouquet formation is thought to contribute to homologue alignment and pairing during first meiotic

prophase (e.g., Therman and Sarto, 1977; Fussell, 1987; Scherthan, 1997; Zickler and Kleckner, 1998).

In *Schizosaccharomyces pombe*, loss of the telomere protein taz1(+) has been shown to abrogate meiotic telomere clustering and to virtually eliminate recombination and ordered disjunction of chromosomes at metaphase I in this asynaptic organism (Cooper et al., 1998; Nimmo et al., 1998). Furthermore, abrogation of nuclear movements during and after telomere clustering impairs chromosome pairing at meiosis (Yamamoto et al., 1999). An essential role for telomeres in the reductional division is underlined by the observation that deletion of telomeres and the resulting rearrangement of linear chromosomes into rings is compatible with vegetative growth, but obstructs meiosis and hence sexual reproduction (Naito et al., 1998; Ishikawa and Naito, 1999).

Numerous cytogenetic studies have shown that a congregation of telomeres occurs in the vicinity of the centrosome or spindle pole body (SPB),[1] during the leptotene/zygotene transition (bouquet formation; for review,

Address correspondence to Harry Scherthan, Dept. of Cell Biology, University of Kaiserslautern, P.O. Box 3049, D-67653 Kaiserslautern, Germany. Tel.: 49 631 205 3313. Fax: 49 631 205 2878. E-mail: scherth @rhrk.uni-kl.de

[1]*Abbreviations used in this paper:* cos, cosmid; FISH, fluorescence in situ hybridization; HA, hemagglutinin; IF, immunofluorescence; SPB, spindle pole body.

see Bélar, 1928; Dernburg et al., 1995; Hiraoka, 1998). Genetic and cytological analyses of the meiotic prophase of *Saccharomyces cerevisiae* have suggested that the formation of a chromosomal bouquet in the synaptic meiosis of budding yeast (Dresser and Giroux, 1988; Trelles-Sticken et al., 1999) occurs independent of homologous recombination and synapsis (Rockmill and Roeder, 1998; Trelles-Sticken et al., 1999). In the vegetative (premeiotic) yeast nucleus, telomeres associate in a few aggregates at the nuclear periphery (Klein et al., 1992; Gotta et al., 1996; Laroche et al., 1998), while centromeres form a single cluster near the SPB (Hayashi et al., 1998; Jin et al., 1998). During the leptotene/zygotene equivalent stage of yeast meiosis, centromeres disperse from the SPB (Hayashi et al., 1998; Jin et al., 1998) and telomeres cluster de novo at this location (Trelles-Sticken et al., 1999). Hence, the bouquet stage of yeast resembles the classical bouquet arrangement formed during prophase I of multicellular eukaryotes (Gelei, 1921; Moens, 1974; Scherthan et al., 1996; Bass et al., 1997).

Genetic analysis of disomic *S. cerevisiae* strains has indicated that telomeres play an important role for homologue search and alignment in synaptic meiosis (Rockmill and Roeder, 1998). The only telomeric protein that has been shown to be involved exclusively in meiosis of budding yeast is Ndj1p/Tam1p (Chua and Roeder, 1997; Conrad et al., 1997). *NDJ1* is expressed specifically after induction of meiosis. Ndj1p-deficient cells show reduced efficacy in homologue disjunction, increased occurrence of nonrecombinant chromosomes (a defect in crossover interference), and a delayed progression through meiotic prophase (Chua and Roeder, 1997; Conrad et al., 1997). Furthermore, spread meiocytes show a disordered distribution of telomeric Rap1p (Conrad et al., 1997). In the present study, we investigate the extent to which bouquet formation, telomere positioning, and chromosome pairing are affected in *ndj1Δ* meiosis and cytologically identify Ndj1p as the first telomeric protein demonstrated to be required for bouquet formation in a synaptic organism.

Materials and Methods

Yeast Strains

To exploit the relatively synchronous progress of SK1 meiosis (Padmore et al., 1991; Trelles-Sticken et al., 1999), the *NDJ1* locus was disrupted in the *S. cerevisiae* SK1 strain (Kane and Roth, 1974) background by replacing the sequence coding for amino acids 13–252 with the KanMX4 cassette (Wach et al., 1994). SK1 yeast transformants resistant to G418 were isolated by A. Goldman and M. Lichten and were assigned the strain name MDY1490 (MATa ura3 lys2 leu2 ho::LYS2 ndj1::KanMX6) and MDY 1493 (MATα ura3 lys2 trp1 ho::LYS2 ndj1::KanMX6). These strains were mated and diploids were selected on the appropriate media (trp−;leu−). Wild-type SK1 haploids (MDY 1484: MATa ura3 lys2 leu2 ho::LYS2; MDY 1487: MATα ura3 lys2 trp1 arg4 ho::LYS2) were mated to result in a diploid wild-type control strain. These strains were used in all fluorescence in situ hybridization (FISH) experiments.

Immunolocalization of telomeres by immunofluorescence to hemagglutinin (HA)-tagged Ndj1p was done in a diploid strain derived from MDY431 and MDY 433 (Dresser et al., 1997).

Cell Culture and Preparation

For nuclear preparation, cultures were grown in presporulation medium to a density of 2×10^7 cells/ml, and then transferred to sporulation medium (2% KAc) at a density of 4×10^7 cells/ml (Roth and Halvorson, 1969). Al-

iquots from the sporulating cultures were obtained during time course experiments at induction of meiosis (transfer to sporulation medium = 0 min) and from 180 to 420 min at 10- or 20-min intervals. Aliquots were immediately transferred to tubes on ice containing 1/10 vol acid-free 37% formaldehyde (Merck). After 30 min, cells were removed from fixative, washed with $1 \times$ SSC and spheroplasted with Zymolyase 100T (100 μg/ml; Seikagaku) in 0.8 M sorbitol, 2% KAc, and 10 mM dithiothreitol. Spheroplasting was terminated by adding 10 vol ice-cold 1 M sorbitol. To allow for the delay in meiotic prophase progression in *ndj1Δ*, we additionally sampled at 5, 6, and 7 h. Spheroplasts were subdivided in two aliquots and subjected either to nuclear spreading (Loidl et al., 1998) or to preparation of structurally preserved nuclei. The latter were obtained as described by Trelles-Sticken et al., (1999) and subjected to FISH.

DNA Probes and Labeling

A composite pancentromeric DNA probe was used to delineate all yeast centromeres (Jin et al., 1998). One plasmid containing a conserved core fragment of the subtelomeric X element and one containing the Y′ element (Louis et al., 1994) were used to probe all yeast telomeres (Gotta et al., 1996; Trelles-Sticken et al., 1999). The following cosmid probes (Fig. 1) were used to determine the pairing of homologous chromosome regions: the telomere-adjacent region on the right arm of *XI* was probed with a cosmid (cos) located at 628.5–665.8 (cos *l*; pUKG066). The smaller chromosomes *IX* and *III* were tagged with cosmid probes hybridizing internally on the left arm of chromosomes *IX* (cos *p*; ATCC 70895) and at HML near the left telomere of chromosomes *III* (cos *m*; ATCC 70884). An internal chromosomes *XI* cosmid (pEKG151, cos *f*; Thierry et al., 1995) mapping 231.8–264.9 on the left arm of chromosomes *XI* was used to monitor meiotic pairing at a telomere-distant chromosomal region (Trelles-Sticken et al., 1999). Chromosome condensation was measured by determining the distance between cosmid *b* (pUKG 040) and cos *h* (pEKG 011) on the left arm of *XI* (Fig. 1; Thierry et al., 1995). Chromosome morphology was monitored by FISH with a painting probe for chromosomes *XI* (Trelles-Sticken et al., 1999), which covers 338 of the 666 kbp large chromosomes *XI* (Dujon et al., 1994).

Probes were labeled either with dig-11-dUTP (Roche Biochemicals) or with biotin-14-dCTP (Life Technologies) using a nick translation kit, according to the supplier's instructions (Life Technologies).

Fluorescence In Situ Hybridization

All preparations were subjected to two-color FISH as described previously (Scherthan et al., 1992; Trelles-Sticken et al., 1999). The hybridization solution contained various differentially labeled probe combinations. It contained the yeast pan-telomere probe, which delineates all telomeres in the SK1 strain (2n = 32) investigated (Jin et al., 1998) and one of the following probes: (a) chromosome-specific cosmid probes (not shown), (b) a chromosomes *XI* paint probe, and (c) a pan-centromeric DNA probe (see Jin et al., 1998). Analysis of pairing of homologous regions was done by two-color FISH to spread nuclei using pairwise combinations of differentially labeled cosmid probes. Immunofluorescent detection of hybrid molecules was carried out with Avidin-FITC (Sigma-Aldrich) and rhodamine-conjugated sheep anti–dig Fab fragments (Roche Biochemicals) (for details, see Scherthan et al., 1992). Before microscopic inspection, preparations were embedded in antifade medium (Vector Laboratories) containing 0.5 μg/ml DAPI (4′6-diamidino-2-phenylindole) as DNA-specific counterstain.

Immunostaining

A polyclonal antiserum against a *S. cerevisiae* spindle pole body component (Tub4; Marschall et al., 1996) was used to stain the SPB in conjunction with telomeres (for details, see Trelles-Sticken et al., 1999). A rabbit antiserum against Zip1p transverse filament protein (Sym et al., 1993; a gift of S. Roeder, Yale University, New Haven, CT) of the yeast synaptonemal complex was applied to identify nuclei with synapsis in progress. Ndj1p was stained in freshly prepared, mildly spread nuclei obtained from a strain that expresses HA-tagged Ndj1p (Conrad et al., 1997) using a monoclonal anti-HA–tag antibody (Biotec Santa Cruz) and secondary anti–mouse Cy3-conjugated antibodies (Dianova).

Rap1p immunostaining of wild-type and *ndj1Δ* diploid cells in the MDY strain background (Dresser et al., 1994) was performed as follows: wild-type and mutant cells were harvested at 4, 7, and 12 h after the shift into sporulation, fixed, spheroplasted, adhered to poly-L-lysine–coated coverslips, and then prepared for immunolabeling by blocking with PBS/
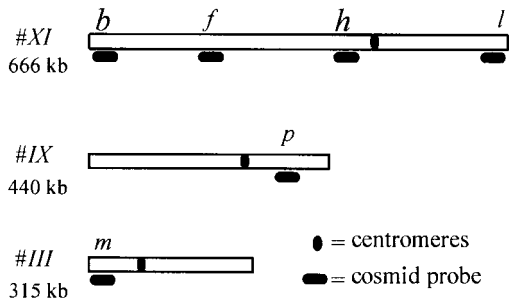
Figure 1. Physical map of chromosomes *III*, *IX*, and *XI* showing the location of the respective cosmid probes used for pairing analysis by FISH (see Materials and Methods for clone numbers).

0.05% Tween 20/4% nonfat dry milk. Preparations of three-dimensionally preserved cells were labeled with a rabbit anti–Rap1p serum (gift of J. Berman, University of Minnesota, St. Paul, MN) diluted 1/10,000, followed by Oregon green-labeled anti–rabbit secondary antibodies (Jackson ImmunoResearch Laboratories), and then mounted with Citifluor anti-fade solution (Ted Pella, Inc.) containing 0.5 µg/ml DAPI under a coverslip.

Microscopic Evaluation

Preparations were evaluated using an epifluorescence microscope (Axioskop; Carl Zeiss, Inc.) equipped with a double band-pass filter for simultaneous excitation of red and green fluorescence, and single band-pass filters for excitation of red, green, and blue (Chroma Technologies). To allow for the evaluation of a large number of nuclei from the time course experiments, investigation of structurally preserved in situ–hybridized nuclei was performed by careful focusing through the nuclei using a 100× plan-neofluoar lens (Carl Zeiss, Inc.). Signal patterns in spread nuclei were investigated with the same set up. Digital images were obtained using a cooled grey-scale CCD camera (Hamamatsu) controlled by the ISIS fluorescence image analysis system (MetaSystems). More than 100 nuclei were scored for each time point and probe combination. Fluorescence signal patterns were analyzed in nuclei with an undisrupted, homogeneous appearance in the DAPI-image.

Confocal Microscopy and Quantitative 3-D Distribution Analysis of Telomeres

Three-dimensionally preserved, Rap1p-stained nuclei were subjected to 3-D microscopy using a Meridian Ultima Z laser-scanning confocal microscope equipped with lasers to image DAPI and fluorescein. Simultaneous two-color scans were made of 10 randomly selected meiotic nuclei from each time point, without regard to the distribution of Rap1p signal, at a pixel and slice step-size of 0.1 µm. An aperture of 100 µm was used with short exposure times to minimize fluorescence fading. Appropriate wavelength scans were made of four fluorescent point source beads (Molecular Probes, Inc.) using the same settings. To avoid any influence of nonrandom telomere clustering that occurs during the bouquet stage, nuclei with less than five signal spots upon visual inspection were excluded from scoring. Averaged point source images were used to deconvolve the experimental images using the freeware *xcosm* v2.1 EM routine (Conchello et al., 1994), mainly to reduce noise in the images, before image analysis.

Image analysis employed Pascal macros running Image (The National Institutes of Health, Bethesda, MD) and free-standing C++ routines written by M.E. Dresser. To measure the distances between the Rap1p spots and the DAPI-defined nuclear periphery: (a) the nuclear periphery was defined by thresholding the DAPI images over a range of different values, where increasingly large values exclude an increasing number of Rap1p spots from the inclusion volume, (b) the coordinates of each Rap1p spot were defined as lying at the center of each distinct signal spot (scored manually using Image and blinded with respect to the location of the nuclear periphery), and (c) the distance between each spot and the threshold-defined periphery was determined by a program that scores the radius of the smallest sphere, centered on the spot, which intersects an "exterior" voxel for spots included in the volume, or which intersects an "interior" voxel for excluded spots; if adjacent, the distance is defined as 0.

To unequivocally determine the relation of the Rap1-FITC signals with the nuclear periphery, we determined the nearest distance from Rap1-FITC signal centers and the nuclear boundary. The latter was determined from the optical section of the DAPI-stained nucleus from the same image plane. All signal spots analyzed were requested to lie with their center in the equatorial plane (within ±0.1 µm of best focus, as determined from the confocal image stacks of sectioned nuclei). The distance of signal gravity centers to the nearest edge of the nucleus was measured using a dedicated program (M.E. Dresser, unpublished data).

Results

Induction of meiosis leads to a dramatic reorganization of yeast nuclear architecture. Centromeres that are tightly clustered at the SPB during vegetative growth disperse throughout the nuclear volume (Hayashi et al., 1998; Trelles-Sticken et al., 1999), while telomeres accumulate de novo at this location (Trelles-Sticken et al., 1999). To determine whether this dramatic reorganization of the early meiotic nucleus requires the Ndj1 protein (Chua and Roeder 1997; Conrad et al., 1997), an *NDJ1* null-mutation (*ndj1Δ*::KanMX4) was introduced into the SK1 strain background because the high synchrony in this strain background facilitates bouquet analysis (Trelles-Sticken et al., 1999). Telomere clustering, centromere distribution, and chromosome pairing were studied by FISH with telomere-, centromere-, and chromosome-specific probes in detergent spread and in three-dimensionally preserved nuclei from meiotic time-course experiments of diploid wild-type and *ndj1Δ* strains. Additionally, using anti–Rap1p signals as marker for meiotic telomeres (Klein et al., 1992; Conrad et al., 1997), telomere positioning with respect to the nuclear periphery was examined by confocal microscopy in the MDY strain background. All experiments analyzed displayed sporulation rates ≥85%.

Dissolution of Premeiotic Centromere and Telomere Clusters Does Not Require Ndj1p

It has been shown that the nuclear organization of vegetative/premeiotic yeast cells is dominated by centromere clustering at the SPB (Fig. 2, a and b), which resolves during the onset of meiotic prophase (Fig. 2, c and d) (Hayashi et al., 1998; Jin et al., 1998). When we determined centromere distribution by FISH to nuclei of SK1 strains, it was found that the frequency of nuclei with one centromere cluster diminished at similar rates after induction of meiosis, both in wild-type and in *ndj1Δ* meiotic time courses (Fig. 3, and not shown). This suggests that dissolution of the centromere cluster is not affected by the absence of Ndj1p.

Premeiotic (vegetative) yeast nuclei usually contain few (two to eight) perinuclear telomere clusters (Klein et al., 1992; Gotta et al., 1996) that are resolved at the onset of meiotic prophase (Fig. 2; Hayashi et al., 1998; Trelles-Sticken et al., 1999). To monitor whether the absence of Ndj1p influences dissolution of vegetative telomere clusters, we determined the fraction of spread nuclei with two to eight telomere clusters at transfer to sporulation medium (0 min) and from 180–420 min, and in undisrupted nuclei at 0 and 180–480 min. Nuclei were also sampled at 530 and 590 min, following the shift into meiosis. It was found that the frequency of spreads with premeiotic telomere distribution (we consider nuclear topology at $t = 0$ to
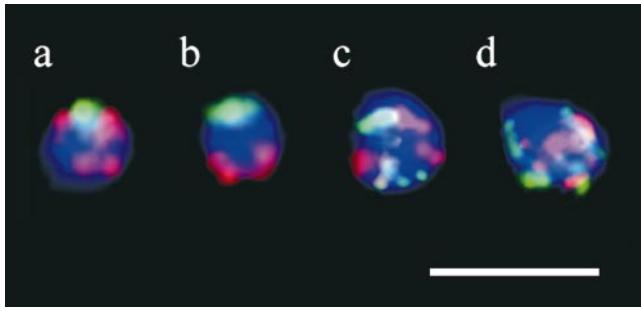
Figure 2. FISH with a pan-centromere probe (fluorescein, green) and a pan-telomere probe (rhodamine, red) to undisrupted diploid nuclei (DAPI, blue) of wild-type and *ndj1Δ* SK1 cells. (a) Vegetative wild-type nucleus before induction of meiosis (*t* = 0 min) displays clustered centromeres that form a single green signal, while telomeres form four perinuclear clusters. (b) Premeiotic *ndj1Δ* nucleus with one centromere cluster and three large telomere clusters at the opposite pole of the nucleus, thereby resembling a Rabl orientation. (c) WT and (d) *ndj1Δ* meiocyte nuclei from two later time points (200 and 260 min, respectively) displaying centromere and telomere signals distributed throughout the nuclei. Few centromere signals are dissociated from the centromere cluster in nucleus (c), while in nucleus (d) exhibits dispersed centromere signals. Bar, 5 μm.

represent premeiotic/vegetative nuclear organization) diminished at similar rates in wild-type and *ndj1Δ* meioses (Fig. 3). Similar results were obtained in repeated time courses and with undisrupted nuclei (not shown). These data suggest the dissolution of premeiotic nuclear archi-

tecture during the onset of sporulation occurs at wild-type rates in the absence of Ndj1p. To further determine whether the *ndj1Δ* mutation affects telomere distribution in vegetative nuclei, we compared telomere FISH signal numbers in 20 randomly selected nuclear spreads obtained during logarithmic vegetative growth in YPD. Spreading of vegetative nuclei dissociates the few clusters seen in intact nuclei to a mean of 22 ± 5 (SD) and to 21 ± 3 telomere signal spots/nucleoid in wild-type and *ndj1Δ* cells, respectively. Similar telomere signal numbers in spread premeiotic wild-type and *ndj1Δ* cells suggest that telomere distribution in vegetative cells is not affected by the *ndj1Δ* mutation, which contrasts with the situation in meiocytes (see below).

NDJ1 Is Required for Meiosis-specific Telomere Distribution

The induction of meiosis leads to the repositioning of telomeres over the nuclear periphery seen as peripheral dispersion of RAP1p-GFP foci in live cells (Hayashi et al., 1998) and by telomere FISH signals in fixed nuclei (Trelles-Sticken et al., 1999). To determine whether the telomere distribution patterns obtained by FISH are representative for meiocytes and to see whether dispersion of meiotic telomeres over the nuclear periphery occurs during sporulation of our strains, we determined the telomere distribution patterns in spread and undisrupted nuclei from time-course experiments after induction of meiosis by FISH with the XY′ telomere probe and performed immunofluorescence (IF) staining of HA-tagged Ndj1p in spread nuclei at *t* = 240 min.
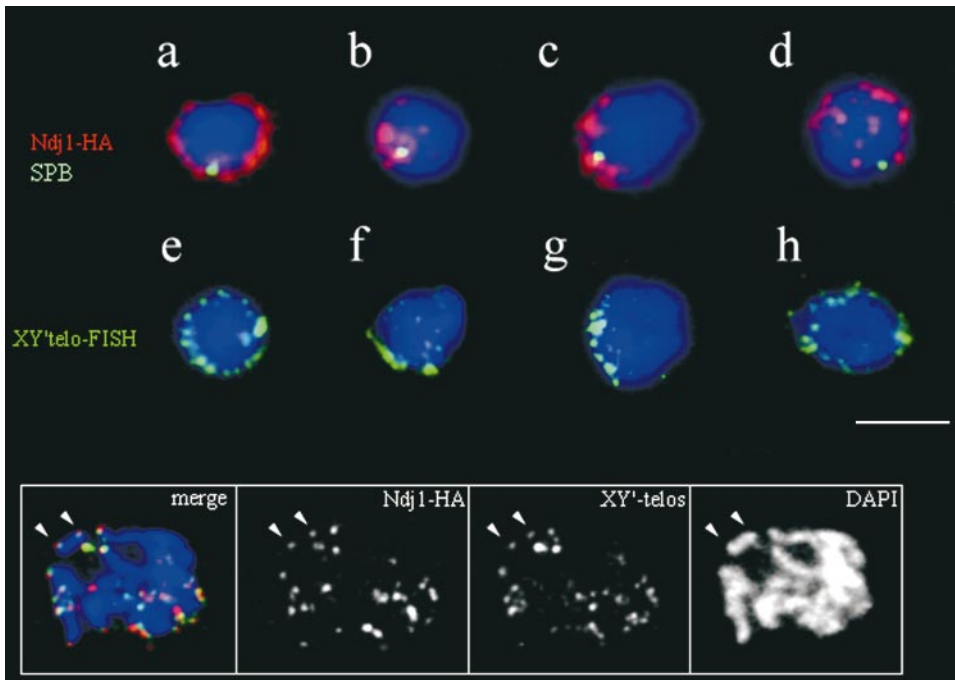

Figure 4. (a–d) Double immunolabeling of SPB components (fluorescein, green) and of meiotic telomeres with antibodies against HA-tagged Ndj1p (rhodamine, red) reveals meiosis-specific telomere distribution patterns in mildly spread diploid wild-type SK1 nuclei. (a) Peripheral rim-like distribution of telomeres during early meiosis (140 min). (b and c) Meiocytes with telomeres accumulated at the SPB (bouquet arrangement). (d) Meiocyte nucleus from a later time point (240 min), which shows an SPB and dispersed telomere signals. (e–h) Mildly spread meiocyte nuclei from an independent FISH experiment with the XY′ repeat probe (see Materials and Methods) reveals telomere patterns similar to the ones obtained by Ndj1p IF. (e) Rim-like telomere distribution. (f and g) Bouquet nuclei with clustered telomere signals. (h) Advanced meiocyte from a later time point displays a scattered telomere distribution. Bar, 5 μm (applies to all details). The inset shows colocalization of Ndj1-HA IF signals (red) and XY′ telo-FISH signals (green) in a wild-type pachytene nucleus. Most of the Ndj1-HA and XY′ signals show significant overlap at chromosome ends (e.g., arrowheads). Ndj1 fluorescence is often seen beyond the telo-FISH signals and/or extends between telomere signals. Fewer IF signals in the Ndj1 channel may relate to loss of some epitopes during the FISH procedure.
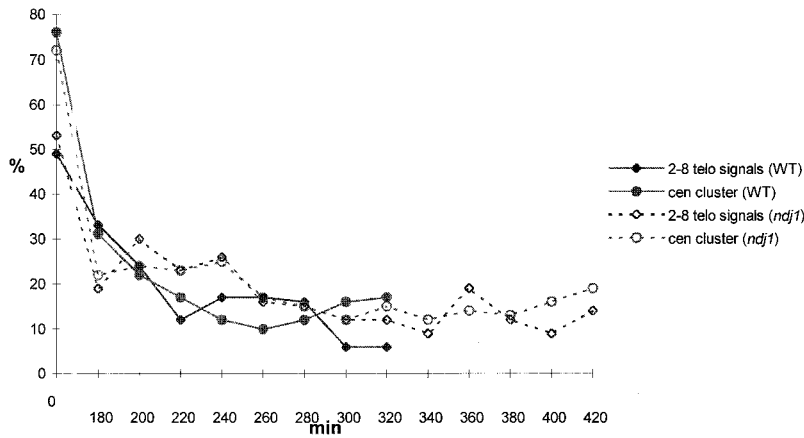
Ndj1p is expressed only during meiosis (Chua and Roeder 1997; Conrad et al., 1997); therefore, the distribution patterns detected with this probe exclusively represent meiotic telomere arrangements. The signal patterns obtained by Ndj1p IF matched the telomere distribution patterns revealed by telo-FISH (Fig. 4). Costaining experiments revealed colocalization of HA-tagged Ndj1p and telomere-FISH signals, with the Ndj1-HA signals often extending beyond the XY′ FISH signals (Fig. 4, inset). This could relate to the abundance of Ndj1p at chromosome ends during meiosis and/or to slight swelling of the epitope-bearing chromatin during the FISH procedure. The lack of IF at some telo-FISH signals may relate to loss of protein during the denaturation and hybridization procedure. In any case, we observed that meiotic telomeres, as marked by FISH as well as with anti–HA-Ndj1p, do adopt a peripheral dispersed arrangement in early meiocytes, which is seen as a rim-like fluorescent signal in mild spreads (Fig. 4, a and e) and at the equatorial focus plane of undisrupted nuclei (not shown). At later time points, telomeres congregate to form a single large signal cluster (bouquet arrangement; Fig. 4, f and g) at the SPB (Fig. 4, b and c). This clustering is resolved as cells enter pachytene

with telomere signals, again becoming dispersed (Fig. 4 d) (Trelles-Sticken et al., 1999).

Nuclei with a rim-like peripheral telomere signal distribution (Fig. 4 a) are rarely encountered at the induction of sporulation, but increase early after induction of meiosis in the wild type (Fig. 5). In contrast, the frequency of spread *ndj1Δ* meiocytes with such a preleptotene-like perinuclear telomere distribution (see Scherthan et al., 1996) essentially remained at a vegetative background level during sporulation, well below the level seen in the wild type (Fig. 5). Similar observations were obtained in time courses of undisrupted *ndj1Δ* nuclei (not shown).

Perinuclear Distribution of Telomeres Is Altered in *ndj1Δ* Meiocytes

To test whether the *ndj1Δ* mutation affects the meiosis-specific three-dimensional telomere distribution (i.e., peripheral location of dispersed telomeres in the meiocyte nucleus), we performed Rap1p staining with undisrupted nuclei and investigated the three-dimensional spot distribution by laser scanning microscopy and digital image analysis. Telomeric Rap1p signal spots and the corre-
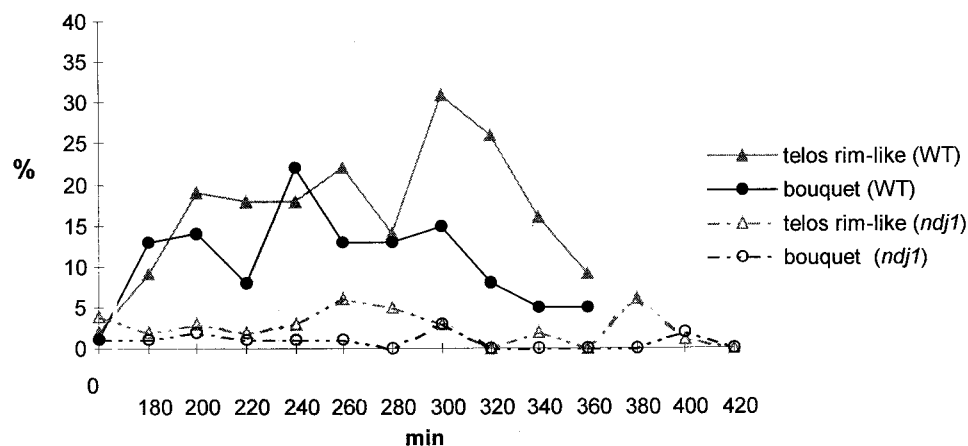
sponding DAPI-stained nuclei were obtained by light optical serial sectioning (Fig. 6). Because nuclei in meiotic prophase are nonspherical and nuclear pore staining failed to reveal the typical rim staining seen in mitotic interphase (not shown), we determined the nuclear boundary in light optical sections of DAPI-stained nuclei. DAPI highly selectively stains DNA and renders the nuclear boundary at a high contrast. The number and relation of Rap1p signal centers to the nearest sector of the nuclear boundary was computed from 30 nuclei of uninucleate cells, 10 each at 4, 7, and 12 h after induction of meiosis from wild type and *ndj1Δ*. Bouquet nuclei, which rarely exceed 5–10% at any time point in this strain background, were excluded from this analysis (see Materials and Methods). The 30 prophase nuclei from wild-type and *ndj1Δ* cells were analyzed as a single class, where totals of 519 and of 729 Rap1p spots were scored, respectively. The difference in the number of total spots is consistent with the smaller number of larger Rap1p signals seen in spread meiotic prophase nuclei of wild type, compared with *ndj1Δ* cells (Conrad et al., 1997).

The relation of the Rap1p telomere signals to the nuclear periphery was determined in the light optical section of the equator of each nucleus. The distance from Rap1/FITC signal centers to the nearest nuclear boundary of the DAPI image was calculated by a dedicated program. This two-dimensional procedure accounts for the small dimensions of the yeast nucleus and its irregular shape at meiosis (see Zickler and Olson, 1975), which precludes applying a distribution analysis of signal spots from a geometrically defined center. The data obtained are displayed in a bar graph according to frequency of signals at distance units of multiples of 0.2 μm from the nearest nuclear boundary segment (Fig. 7). In wild-type cells, the vast majority of telomeric spots were found near the nuclear periphery (Figs. 6 and 7). A deviation from this peripheral telomeric Rap1p distribution in wild-type meiocyte nuclei was apparent in *ndj1Δ* nuclei. In the latter, a significant fraction of signals (97.5% level by G test) located remote from the nuclear boundary (i.e., 34% of signal spots were located 0.6–1 μm from the nearest nuclear edge), while in the wild type only 18% of spots were found in this more internal nuclear compartment (Fig. 7). These results suggest that the perinuclear localization of meiotic telomeres is disrupted in *ndj1Δ* meiosis.

Ndj1p Is Essential for Formation of the Bouquet

In the SK1 background, we observed that the premeiotic telomere distribution is resolved in diploid *ndj1Δ* cells at wild-type rates. However, a rim-like perinuclear telomere distribution was detected only at insignificant rates (Fig. 5). This prompted us to also determine the frequency of meiocytes with a single telomere-FISH signal cluster, a telomere distribution diagnostic for a chromosomal bouquet (Fig. 4, f and g) that transiently forms at the leptotene/zygotene transition during prophase I of *S. cerevisiae* (Trelles-Sticken et al., 1999). Induction of meiosis in the wild type led to a 22-fold increase in the frequency of mildly spread nuclei with a single telomere cluster over premeiotic background at *t* = 240 min (Fig. 5). In undisrupted nuclei, a 5.3-fold increase at 260 min (not shown) was noted, which is well in agreement with earlier observa-
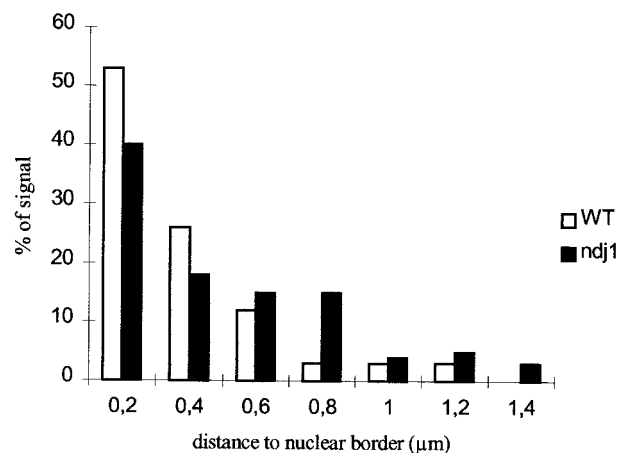

Figure 7. Spatial analysis of Rap1p telomere signal distribution with respect to the nearest nuclear boundary segment. The frequency (%) of occurrence of Rap1/FITC signal centers situated at particular distances (given in 0.2-μm intervals) from the nearest nuclear periphery segment as determined at the equatorial plane from the corresponding confocal DAPI images. The values were derived from 146 signal spots for *ndj1Δ* (ndj1), and 86 for wild type (WT). In the wild type, most signal spot centers locate in the immediate vicinity of the nuclear periphery (open bars). An altered spatial distribution of telomeric Rap1 signals in *ndj1Δ* nuclei is reflected by a higher portion of telomeric signals being more distant from the nuclear border (solid bars).

tions in undisrupted wild-type SK1 meiocytes (Trelles-Sticken et al., 1999).

A severe deviation from the wild-type situation was observed in *ndj1Δ* meiosis. The frequency of nuclei with a single telomere cluster never exceeded premeiotic levels, even in time courses with prolonged duration and in time-course experiments where we performed FISH to intact meiocyte nuclei (Fig. 5, and not shown). The defect in telomere clustering was also evident when telomere FISH signal numbers were compared in 20 randomly selected wild-type and mutant nuclei. Spread *ndj1Δ* meiocytes (obtained 300 min after induction of meiosis) contained a significantly increased spot number/nucleus as compared with wild-type meiocytes that were sampled at 200 min to compensate for the delay in mutant prophase I (Fig. 8). Similar results were obtained using anti–Rap1p IF and confocal microscopy (data not shown).

Since formation of a true bouquet involves telomere clustering at the SPB during the leptotene/zygotene transition stage (Trelles-Sticken et al., 1999), we determined whether SPB/telomere cluster association is absent in *ndj1Δ* meiocytes. To this end, we simultaneously immunostained for spindle pole body and telomeres by FISH in intact nuclei at 240 min in wild-type and mutant meiosis. We failed to detect a physical association of the SPB signal and XY′ telomeric signal accumulations seen in a few *ndj1Δ* nuclei (not shown). This and the constant and negligible frequency of nuclei with a single telomere-FISH signal cluster over mutant time courses corroborates that bouquet formation is impaired in *ndj1Δ* meiosis. To further investigate whether telomere clustering is defective during the leptotene/zygotene transition stage, we immunostained spread meiocytes with antibodies to Zip1p, a
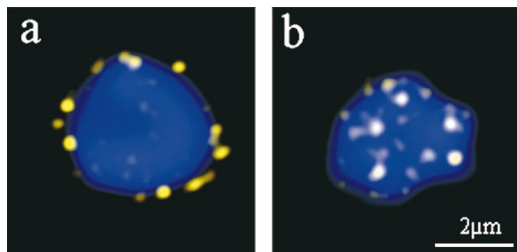
Figure 6. Confocal light optical sections at the equatorial planes of (a) a wild-type (taken at 240 min) and (b) an *ndj1Δ* nucleus (taken at 470 min) showing telomere-associated Rap1 signals (FITC, yellow) and DNA fluorescence (DAPI, blue). In the wild-type nucleus (a), telomeric Rap1p signals are confined to the nuclear periphery. The *ndj1Δ* meiocyte nuclear section (b) shows telomeric Rap1p signals at the periphery and within the nuclear interior. Bar, 2 μm.

component of transverse filaments of the synaptonemal complex (Sym et al., 1993) and determined the telomere distribution by FISH in SK1 meiocytes, obtained at $t = 200$ min with an incomplete speckled Zip1p distribution, which represent nuclei with synapsis in progress. It was found that telomere signals were scattered throughout mildly spread *ndj1Δ* nuclei ($n = 168$; obtained at 300 min) with a fragmented Zip1p distribution (zygotene-equivalent stage; Fig. 9, a–c), while in the wild type 20% of zygotene cells ($n = 166$) contained a single telomere cluster (see also Trelles-Sticken et al., 1999). These data suggest that true bouquet formation is disrupted in *ndj1Δ* meiosis.

Zip1p IF disclosed furthermore that *ndj1Δ* nuclei contained an unusually high frequency of intensely staining Zip1-positive structures that have been called "polycomplexes" (Sym and Roeder, 1995). At 210 min after induction of meiosis, 81% of *ndj1Δ* nuclei contained predominantly one Zip1 polycomplex (PC) in the form of a brightly stained rod (Fig. 9, a and b), while at this time point only 28% of wild-type nuclei contained a PC. This
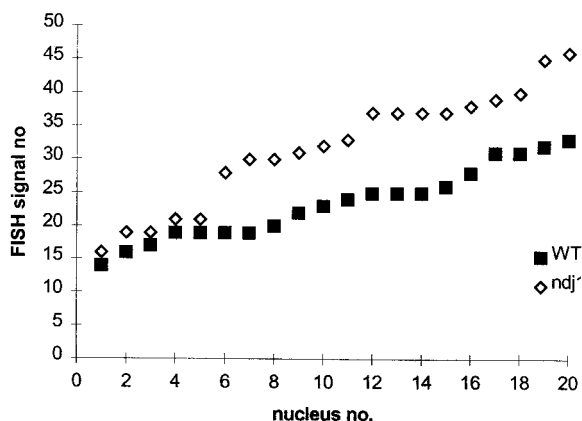

Figure 8. Analysis of telomere FISH signal numbers in 20 randomly selected, mildly spread nuclei of diploid SK1 wild-type and *ndj1Δ* meiocytes. Nuclei were obtained 200 and 300 min after induction of meiosis in the wild type and *ndj1Δ*, respectively, to allow for a compensation of the delay in mutant prophase I. Ranking according to increasing numbers of telomere FISH signals/nucleoid reveals that *ndj1Δ* meiocytes display significantly larger telomere signal numbers/nucleus.
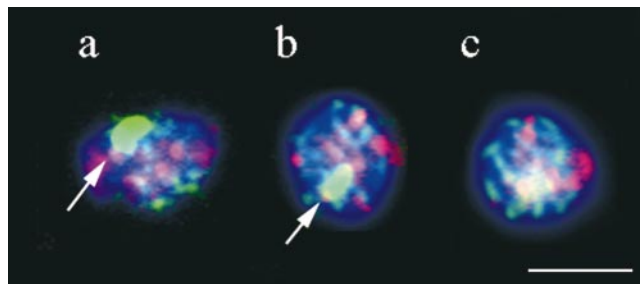

Figure 9. Costaining of telomeres by FISH (rhodamine, red) and Zip1p by IF (FITC, green) in mildly spread *ndj1Δ* meiocyte nuclei (DAPI, blue). (a and b) Spread nuclei (obtained at 210 min after induction of meiosis) display Zip1-signal stretches and a Zip1 polycomplex (bright green oblong, arrow), while telomere FISH signals are dispersed. (c) Nucleus with dispersed telomeres but without Zip1 polycomplex from a later time point (330 min). Bar, 5 μm.

represents an approximately threefold increase of PCs in the mutant. At 330 min, 60% of *ndj1Δ* meiocytes still contained PCs, while these were absent in the wild type. In yeast meiosis, formation of Zip1 polycomplexes has been observed in a variety of conditions and strain backgrounds (see Sym and Roeder, 1995). An increased frequency of PCs is often seen in recombination mutants, which generally show defects in synapsis (e.g., Alani et al., 1990; Loidl et al., 1994; Sym and Roeder 1995; Grushcow et al., 1999). Taken together, these data suggest that normal synaptic progression requires Ndj1p and bouquet formation.

Chromosome Pairing Is Impeded in ndj1Δ Meiosis

Since a mutant with disrupted bouquet formation offers the possibility to test for the impact of meiotic telomere clustering for the homologue pairing process, we investigated homologue pairing by FISH with cosmid probes to regions on chromosmes *III*, *IX*, and *XI* (Fig. 1) during wild-type and mutant sporulation. While chromosomes *XI* represents a large chromosome that is capable spanning the entire nuclear volume, *IX* is of intermediate size, and *III* is among the smallest yeast chromosomes. Due to the clustering of vegetative centromeres at the spindle pole body (Hayashi et al., 1998, Jin et al., 1998) and other functions, the yeast nucleus displays a substantial amount of premeiotic homologue association (Loidl et al., 1994;
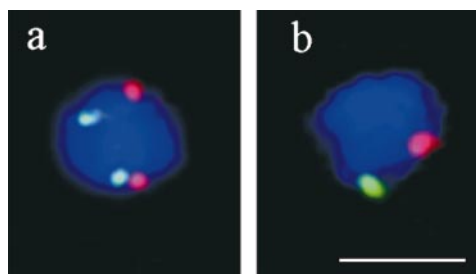

Figure 10. Two-color FISH with cosmid probes *m* (*III*, green) and *p* (*IX*, red) to spread nuclei of SK1 meiocytes. Nuclei were taken at $t = 180$ min. (a) Spread nucleus with cosmid signals apart. (b) Meiocyte with both pairs of homologous cosmid signals paired. Therefore, the signals appear enlarged. Bar, 5 μm.

Weiner and Kleckner, 1994; Burgess et al., 1999). Pairing interactions are disrupted during premeiotic S-phase, and then return at meiosis-specific levels that well exceed vegetative levels (Loidl et al., 1994; Weiner and Kleckner 1994; Nag et al., 1995; Trelles-Sticken et al., 1999). In the present investigation, pairing of homologous chromosome regions was determined by FISH of two differentially labeled cosmid probes to two-dimensional nuclear spreads that yields two signals pairs in the same focal plane. Spreading has been shown to enhance cytological resolution in the unfavorably small yeast nucleus and to dissociate weak chromosome interactions while leaving stable interactions intact (see Weiner and Kleckner, 1994; Nag et al., 1995; Jin et al., 1998). We regarded homologous regions paired when cosmid signals of the same color were touching each other or formed an enlarged confluent signal (Fig. 10 b). To ensure saturated target regions, only nucleoids containing strong signals of both colors were analyzed. Two-color FISH with cosmid pairs *f/l* and *m/p* (see Figs. 1 and 10) was performed on nuclear spreads obtained from meiotic time courses of *ndj1Δ* and wild-type cells. In initial experiments, we determined the frequencies of associations between heterologously colored signals, which provides a measure for accidental signal contacts. Both wild-type and mutant time courses displayed nearly identical frequencies of heterologous signal associations at 0, 3, 5, and 7 h in sporulation. Specifically, at all time points, the mean fraction of successfully hybridized spreads showing heterologous signal contacts for cosmid combinations *f/l* and *m/p* was 8.5% (range 7.3–8.9) and 9.3% (range 9–10.2), respectively. These values are well in agreement

with estimations reported by others (see Burgess et al., 1999). To adjust for accidental contacts between cosmid signals, which may be influenced by a number of parameters (see above), we used centromere distant probes and furthermore subtracted 50% of the obtained fraction showing heterologous contacts from the obtained pairing values, since in two cosmid FISH experiments a signal has a two- to fourfold higher probability to be associated with a heterologous than with a homologous signal. It should be noted that the results obtained with and without such a correction remained essentially the same (not shown).

In wild-type and *ndj1Δ* time courses, the fraction of nucleoids with FISH signals homologously paired increased well above premeiotic values (Fig. 11). In *ndj1Δ* meiosis, all homologous regions investigated reached nearly wild-type levels of homologous signal pairing, but with a 2–3-h delay (Fig. 11). This slowed progression of homologous pairing is mirrored by a 2-h delay in the appearance of anaphases I and II in *ndj1Δ* meiosis as compared with the wild type, where these first appeared at 300 and 320 min, respectively (not shown, consistent with earlier reports). In wild-type meiosis, the homologous region near the left telomere of the small chromosomes *III* paired most rapidly (Table I). However, in the absence of Ndj1p and bouquet formation, the telomeric region of chromosomes *III* showed the most prominent retardation of homologous pairing, expressed as the difference in time required in wild-type and *ndj1Δ* meiosis to reach peak values in signal pairing ($\Delta t = 160$ min, Fig. 11). Pairing of the telomeric region of the right arm of the large chromosomes *XI* (cos l), in contrast, showed only a delay of 100 min in *ndj1Δ* meiosis. Pairing of large chro-
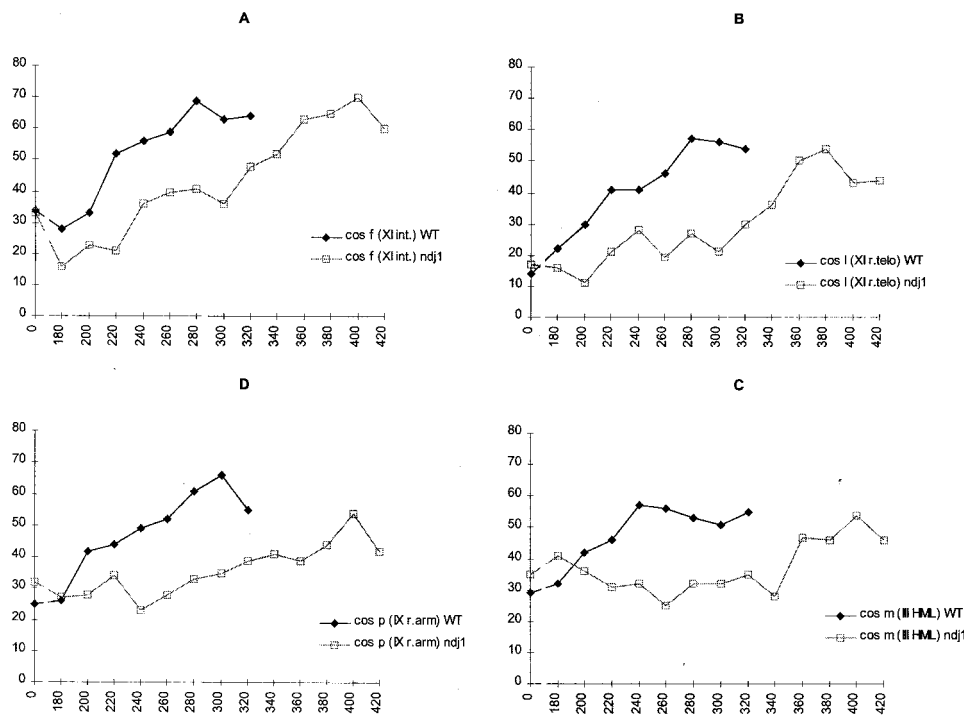

Figure 11. FISH analysis of homologue pairing during meiotic time courses of wild-type and *ndj1Δ* SK1 strains. Cosmid probe combinations *m/p* and *f/l* were hybridized to spread preparations obtained at the respective time points (minutes). Pairing values were obtained by determining the fraction of nuclei containing cosmid signals of the same color that touched each other or showed an enlarged coalesced signal. More than 200 FISH signal pairs were scored per time point, probe combination, and strain. Values were corrected for accidental heterologous contacts by subtracting 5% for cosmid combination *m/p* and 4% for probe combination *l/f* (see text). (A) Frequencies of nuclei with paired cos *f* signals (*XI* internal; Fig. 1) in wild-type (WT) and *ndj1Δ* (ndj1) time courses. (B) Frequencies (%) of paired cos l (*XI,* right telo) in wild-type and *ndj1Δ* time courses. (D) Frequencies of nuclei with paired cos *p* signals (*IX,* right arm) in wild-type and *ndj1Δ* time courses. (C) Frequencies of nuclei with paired cos *m* signals (*III,* HML) in wild-type and *ndj1Δ* time course. At all loci probed, the frequencies of nuclei with paired signals increase more gradually in the absence of Ndj1p, reaching nearly wild-type frequencies with a 2–3-h delay. In the wild type, signal patterns are displayed only until 320 min, since meiotic divisions (anaphases) appeared after 300 min and complicated the signal analysis.

Table I. Retardation of Homologue Pairing if ndj1Δ Meiosis

Cosmid probe	Maximal signal pairing in WT at t	Maximal signal pairing in ndj1Δ meiosis at t	Δt
	min	*min*	*min*
Cos m (*III* HML)	240	400	160
Cos p (*IX*, right arm)	300	400	100
Cos f (*XI*, interstitial)	280	400	120
Cos l (*XI*, right telo)	280	380	100

Time taken in wild-type and *ndj1Δ* meiosis to reach peak values in homologous FISH-signal pairing (minutes). Δt, time difference between the peak homologue pairing values for a given cosmid probe in wild-type and *ndj1Δ* meiotic time courses.

mosomes may thus be less dependent on a catalytic action of telomere clustering on homologue pairing, since these may span the entire nucleus and therefore have a higher probability for chance encounters with their homologues in the absence of bouquet formation.

Condensation of Chromosome Territories Occurs in the Absence of Ndj1p

Previous chromosome painting studies have shown that yeast chromosomes extend, pair, and condense during the course of meiotic prophase (Scherthan et al., 1992; Trelles-Sticken et al., 1999). To test whether the *ndj1Δ* mutation influences this morphological change of yeast chromosomes during meiosis, we painted chromosomes *XI* in conjunction with telomere FISH in wild-type and *ndj1Δ* cells at 180, 240, 360, and 420 min after induction of meiosis. Nuclei with all aspects of meiotic chromosome morphology were detected in wild-type and *ndj1Δ* cells (Fig. 12). The painting of yeast chromosomes also allows chromatin condensation to be assessed. The fraction of uninucleated meiocytes that exhibit clear and compact FISH signals represents the fraction of cells in which chromosomes are condensed (pachytene; Scherthan et al., 1992; Loidl et al., 1994; Nag et al., 1995). The frequency of condensed *XI* pachytene bivalents was determined in uninucleate mutant and wild-type SK1 meiocytes (Fig. 12 d). In *ndj1Δ* meiosis, chromatin condensation was found to be significantly delayed with respect to wild type (Fig. 13), although chromosome condensation per se is not affected by the

ndj1Δ mutation. Thus, chromosome condensation was further monitored by FISH with differentially labeled cosmid probes *b* and *l* in uninucleated meiocytes obtained at t = 240 min in wild type and t = 360 min in *ndj1Δ* time courses. Cosmids *b* and *l* map to the proximal and distal part of the left (long) arm of *XI* (Fig. 1). The distance between the centers of the paired and differentially colored cosmid signals on pachytene bivalents was determined in 30 randomly selected spread nuclei. The mean distance observed between the two cosmid signals was 1.1 ± 0.4 μm (±SD) in the wild type and 1.0 ± 0.4 μm in *ndj1Δ* nuclei. The difference between the two data sets did not differ significantly (P = 0.23 at 0.01; Student's *t* test). This further suggests that chromosome condensation is not affected by the absence of Ndj1p.

Discussion

Ndj1p May Be Required for Peripheral Localization of Meiotic Telomeres

Chromosome topology of the vegetatively growing yeast is dominated by tightly clustered centromeres next to the spindle body (Hayashi et al., 1998; Jin et al., 1998) and by telomeres forming a few aggregates at the nuclear periphery (Klein et al., 1992; Gotta et al., 1996). Upon induction of meiosis, nuclear topology is reorganized. Centromeres become dispersed throughout the nucleus, and telomeres spread over the nuclear periphery (Hayashi et al., 1998), except during an intermediate stage when telomeres form a tight cluster in the vicinity of the spindle pole body; i.e., at the bouquet stage (Trelles-Sticken et al., 1999).

Two of the early steps in the meiotic nuclear reorganization, dispersion of centromeres and telomeres, apparently are unaffected by deletion of *NDJ1*. However, this close proximity of dispersed telomeres to the nuclear periphery, which is evident in wild-type cells (Hayashi et al., 1998, and this report) does appear defective in *ndj1Δ*. During earliest meiotic prophase, telomeres dissociate from the vegetative aggregates and line the nuclear periphery (Fig. 14), giving raise to a rim-like staining in ∼20% of wild-type nuclei, which resembles the telomere distribution
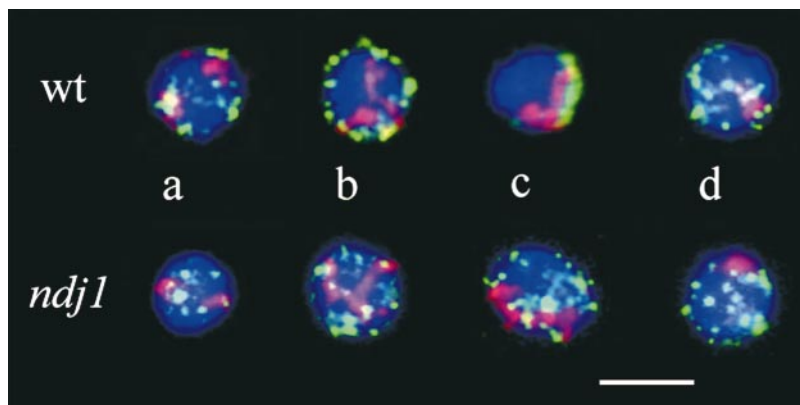

Figure 12. Representative images of FISH signal patterns obtained with a painting probe for chromosomes *XI* (red) and the pan-telomere probe (green) in mildly spread nuclei from meiotic time courses of diploid wild type (wt) and *ndj1Δ* (*ndj1*) SK1 strains (a, 0 min; b and c, 260 min; d, 380 min). Images are aligned according to meiosis-specific changes in chromosome morphology during prophase I (see Trelles-Sticken et al., 1999). (a) Premeiotic wild-type and *ndj1Δ* nuclei (0 min) display separated variably shaped chromosomes *XI* territories and several telomere clusters. (b, wt*)* WT meiocyte nucleus with extended chromosome *XI* signal tracks and a rim-like distribution of telomere signals. (b, *ndj1*) Meiocyte with scattered telomere signals, while *XI* signal tracks extend across the nucleus and touch at one end. (c, wt) Nucleus with one large telomere signal cluster (bouquet arrangement). Chromosomes *XI* form one outstretched signal track along the telomere cluster. (c, *ndj1*) *ndj1Δ* meiocyte with scattered telomeres. Painted chromosomes *XI* are seen as a single extended signal track. (d) Wild-type and mutant pachytene nuclei both exhibit a condensed *XI* bivalent and scattered telomeres. Bar, 5 μm.
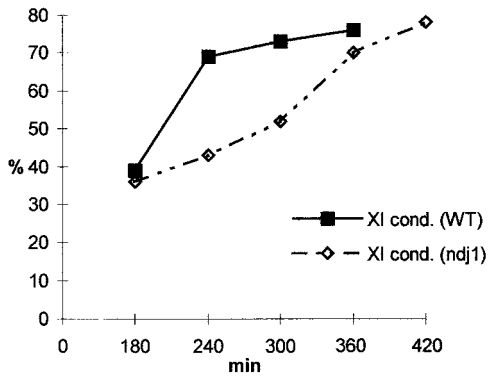
Figure 13. Frequency (%) of uninucleate meiocytes with condensed chromosome *XI* bivalent (Fig. 12 d) at given time points (minutes) in wild-type (WT) and *ndj1Δ* (ndj1) meiosis in the SK1 background. In *ndj1Δ* meiosis, the frequency of uninucleated meiocytes with a condensed *XI* bivalent increased more gradually than in the wild type.

seen in the late preleptotene/leptotene stage of mammalian prophase I (Scherthan et al., 1996). In mammals, the switch from premeiotic to meiotic telomere distribution is a two-step process, with telomeres first attaching at scattered points over the nuclear envelope, and then congregating in the bouquet to a limited sector of the nuclear envelope (Rasmussen and Holm, 1978; Boiko, 1983; Scherthan et al., 1996). In *ndj1Δ* meiosis of yeast, FISH and IF analyses of telomere distribution in undisrupted and mildly spread nuclei revealed a paucity of nuclei with telomeres lining the nuclear periphery and a concomitant increase in the frequency of nuclei with telomeres scattered throughout the nuclear lumen, as inferred from three-dimensional Rap1p analysis. These observations indicate that the absence of Ndj1p impairs the assembly of a meiosis-specific perinuclear telomere topology (Fig. 14) after dissolution of the few vegetative telomere clusters

(see Gilson et al., 1993). Furthermore, these observations indicate that localization of telomeres to the nuclear periphery requires Ndj1p, in accord with speculation based on an earlier genetic analysis of *NDJ1/TAM1*-deficient cells (Chua and Roeder, 1997). Localization of the ends of yeast synaptonemal complexes to the nuclear envelope has been demonstrated by electron microscopy (Byers and Goetsch, 1975; Zickler and Olson, 1975; Moens and Ashton, 1985) and a similar analysis of *ndj1Δ* is underway (Z. Zhang, M.N. Conrad, and M.E. Dresser).

Bouquet Formation Facilitates Homologue Interaction

Distribution of recombination events (crossover interference), chromosome segregation, and distributive disjunction (Chua and Roeder, 1997; Conrad et al., 1997) are all affected by deletion of *NDJ1* but, for the major part, the defects are relatively mild and may arise from a telomere-related delay in meiotic prophase (Chua and Roeder, 1997). The delay in onset and completion of synapsis (Conrad et al., 1997) potentially is due to a defect in some aspect of chromosome pairing that normally brings homologues into close apposition for the initiation of homosynapsis. FISH in conjunction with Zip1p immunostaining showed that telomeres fail to cluster during the leptotene/zygotene-equivalent stages, when bouquet formation normally occurs (Dernburg et al., 1995; Zickler and Kleckner, 1998). Moreover, the meiotic SPB failed to show an association with a telomere accumulation occasionally seen in Ndj1-deficient nuclei. This suggests that loss of bouquet formation is the underlying defect of the retarded synapsis progression and chromosome pairing in the *ndj1Δ* mutant (see below).

When we investigated homologue pairing at four regions on three chromosomes by two-color cosmid FISH, a highly significant reduction in chromosome pairing was noted at time points in mutant meiosis when, in the wild type, signal pairing had reached its maximum. Prolonged time courses in the *ndj1Δ* mutant showed that there is a
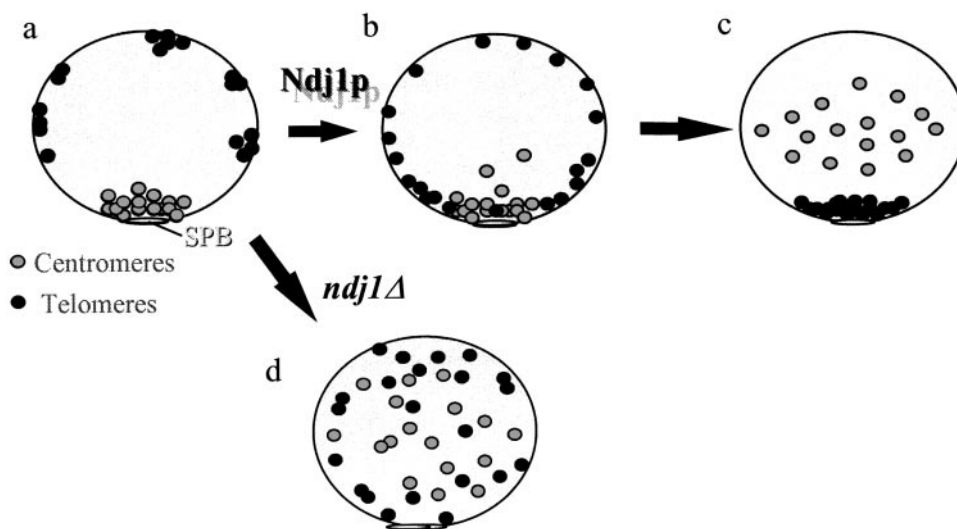

Figure 14. Scheme showing the sequential steps of centromere and telomere redistribution that occur during earliest meiotic prophase of yeast. It is based on the observations made in this and earlier reports (see text). (a) In the premeiotic nucleus, telomeres (black) and centromeres (gray) form several telomere and one centromere cluster at the nuclear periphery. (b) In the wild type, induction of meiosis leads to dissolution of the centromere cluster and perinuclear telomere clusters. Centromeres become dispersed throughout the nuclear lumen, while telomeres disperse over the nuclear periphery. (c) Bouquet stage: telomeres tightly cluster at the spindle pole body, while centromeres are dispersed. (d) While premeiotic telomere topology is not affected, the early steps of meiotic telomere redistribution appear defective in the absence of Ndj1p, which leads to scattering of both telomeres and centromeres throughout the *ndj1Δ* meiocyte nucleus.

2–3-h delay in chromosome pairing. A similar delay was noted for the compaction of chromosomes *XI* bivalents, but, ultimately, chromosome condensation as measured by cosmid FISH appeared normal. When we compared the time required for the homologous regions assayed to reach meiosis-specific values in wild-type and *ndj1Δ* meiosis, it appeared that the pairing of the telomeric regions of the relatively small chromosomes *III* was most severely delayed. In Ndj1p-deficient meiosis, the left telomere region on chromosomes *III* took 60 min longer to reach peak-pairing values than the telomeric region of the right arm of the large chromosomes *XI* and on chromosomes *IX*. This may indicate that smaller chromosomes are more dependent on the action of telomere clustering to instigate homologue alignment and pairing. However, after a delay of ~2–3 h, all homologous regions investigated reached approximately wild-type pairing values, which shows that telomere-independent routes of homologue pairing exist. Altogether, it appears that bouquet formation is not required for homologue recognition and synapsis per se, but mediates an important catalytic action on homologue pairing, which shortens the duration of sporulation, and thus may, in turn, confer selective advantages in a natural environment. This conclusion is in agreement with long-standing hypotheses that telomere clustering during the bouquet stage facilitates homologue interactions by aligning chromosome ends (for reviews, see Rhoades, 1961; Moses, 1968; Scherthan, 1997; de Lange, 1998b; Zickler and Kleckner, 1998).

Furthermore, there is supporting experimental evidence from *S. pombe* (Chikashige et al., 1997) where, in analogy to the situation in budding yeast *ndj1Δ* mutants, absence of the telomere protein Taz1p(+) abrogates telomere clustering and leads to reduced recombination and increased meiotic nondisjunction in fission yeast (Cooper et al., 1998; Nimmo et al., 1998). Thus, the primary, important consequence of deletion of *NDJ1* is likely to be the failure of bouquet formation, with the subsequent defects arising from distorted telomere distribution and the absence of bouquet-facilitated homologue alignment and pairing, as suggested based on genetic data from disomic synaptic meiosis (Rockmill and Roeder, 1998). The *ndj1Δ*-related delay may result from overloading of the homology testing machinery due to disordered chromosome distribution in the absence of meiotic telomere clustering. Dissolution of premeiotic/vegetative centromere and telomere aggregates at the onset of meiosis may still create sufficient chromosome movement in the Ndj1p-deficient prophase nucleus for portions of chromosomes to make contact and, once partially aligned, to commence with homosynapsis. Particularly, larger-sized chromosomes may benefit from an increased probability of encountering a portion of its homologue and to initiate stable pairing earlier than smaller ones. Synapsis, which may initiate at a few interstitial sites (Dresser and Giroux, 1988; Rockmill et al., 1995; Chua and Roeder, 1997; Trelles-Sticken et al., 1999) seems to proceed at a slower rate in the *ndj1Δ* mutant, since Zip1p polycomplexes resolve more gradually. Jumbled telomere localization and nonsynchronized homologue pairing may be the cause for defective crossover interference in the absence of Ndj1p (see Chua and Roeder, 1997). However, at the present state, it cannot be excluded that the *ndj1Δ* phenotypes result from other so far unknown effects besides the telomeric ones.

An interesting possibility is that Ndj1p may link meiotic telomeres to motor proteins at the nuclear envelope, the action of which is thought to bring about telomere aggregation during the bouquet stage (see Bascom-Slack and Dawson, 1997; Zickler and Kleckner, 1998). Future research will have to show whether perinuclear filaments, like the Mlp proteins (Strambio-de-Castillia et al., 1999), which are involved in tethering vegetative telomeres to nuclear pore complexes (Galy et al., 2000), also play a role in telomere clustering during meiotic prophase.

References

Alani, E., R. Padmore, and N. Kleckner. 1990. Analysis of wild-type and rad50 mutants of yeast suggests an intimate relationship between meiotic chromosome synapsis and recombination. *Cell.* 61:419–436.

Bass, H.W., W.F. Marshall, J.W. Sedat, D.A. Agardand, and W.Z. Cande. 1997. Telomeres cluster de novo before the initiation of synapsis: a three-dimensional spatial analysis of telomere positions before and during meiotic prophase. *J. Cell Biol.* 137:5–18.

Bélar, K. 1928. Chromosomenreduktion. *In* Handbuch der Vererbungswissenschaft, die Cytologischen Grundlagen der Vererbung. E. Baur and M. Hartmann, editors. Geb. Borntraeger, Berlin. 168–201.

Bascom-Slack, C.A., and D.S. Dawson. 1997. The yeast motor protein, *Kar3p*, is essential for meiosis I. *J. Cell Biol.* 139:459–467.

Blackburn, E.H. 1991. Structure and function of telomeres. *Nature.* 350:569–573.

Burgess, S.M., N. Kleckner, and B.M. Weiner. 1999. Somatic pairing of homologs in budding yeast: existence and modulation. *Genes Dev.* 13:1627–1641.

Byers, B., and L. Goetsch. 1975. Electron microscopic observations on the meiotic karyotype of diploid and tetraploid *Saccharomyces cerevisiae. Proc. Natl. Acad. Sci. USA.* 72:5056–5060.

Boiko, M. 1983. Human meiosis VIII. Chromosome pairing and formation of the synaptonemal complex in Oocytes. *Carlsberg Res. Commun.* 48:457–483.

Chikashige, Y., D.-Q. Ding, Y. Imai, M. Yamamoto, T. Haraguchi, and Y. Hiraoka. 1997. Meiotic nuclear reorganization: switching the position of centromeres and telomeres in the fission yeast *Schizosaccharomyces pombe. EMBO (Eur. Mol. Biol. Organ.) J.* 16:193–202.

Chua, P.R., and G.S. Roeder. 1997. Tam1, a telomere-associated meiotic protein, functions in chromosome synapsis and crossover interference. *Genes Dev.* 11:1786–1800.

Conrad, M.N., A.M. Dominguez, and M.E. Dresser. 1997. Ndj1p, a meiotic telomere protein required for normal chromosome synapsis and segregation in yeast. *Science.* 276:1252–1255.

Conchello, J.A., J.J. Kim, and E.W. Hansen. 1994. Enhanced three-dimensional reconstruction from confocal scanning microscope images. II. Depth discrimination versus signal-to-noise ratio in partially confocal images. *Appl. Opt.* 33:3740–3750.

Cooper, J.P., Y. Watanabe, and P. Nurse. 1998. Fission yeast Taz1 protein is required for meiotic telomere clustering and recombination. *Nature.* 392:828–831.

de Lange, T. 1998a. Telomeres and senescence: ending the debate. *Science.* 279:334–335.

de Lange, T. 1998b. Ending up with the right partner. *Nature.* 392:753–754.

Dernburg, A.F., J.W. Sedat, W.Z. Cande, and H.W. Bass. 1995. The cytology of telomeres. *In* Telomeres, E.H. Blackburn and C.W. Greider, editors. Cold Spring Harbor Laboratory Press, Cold Spring Harbor, NY. 295–338.

Dresser, M.E., and C.N. Giroux. 1988. Meiotic chromosome behavior in spread preparations of yeast. *J. Cell Biol.* 106:567–573.

Dresser, M.E., D.J. Ewing, S.N. Harwell, D. Coody, and M.N. Conrad. 1994. Nonhomologous synapsis and reduced crossing over in a heterozygous paracentric inversion in *Saccharomyces cerrevisiae. Genetics.* 138:633–647.

Dresser, M.E., D.J. Ewing, M.N. Conrad, A.M. Dominguez, R. Barstead, H. Jiang, and T. Kodadek. 1997. DMC1 functions in a *Saccharomyces cerevisiae* meiotic pathway that is largely independent of the RAD51 pathway. *Genet-*

ics. 147:533–544.

Dujon, B., D. Alexandraki, B. André, W. Ansorge, V. Baladron, J.P. Ballesta, A. Banrevi, P.A. Bolle, M. Bolotin-Fukuhara, P. Bossier, et al. 1994. Complete DNA sequence of yeast chromosome XI. *Nature*. 369:371–378.

Fussell, C.P. 1987. The Rab1 orientation: a prelude to synapsis. *In* Meiosis. P.B. Moens, editor. Academic Press, Inc., Orlando, FL. 275–299.

Galy, V., J.C. Olivo-Marin, H. Scherthan, V. Doye, N. Rascalou, and U. Nehrbass. 2000. Nuclear pore complexes in the organization of silent telomeric chromatin. *Nature*. 403:108–112.

Gelei, J. 1921. Weitere Studien über die Oogenese des *Dendrocoelum lacteum*. III. Die Konjugation der Chromosomen in der Literatur und meine Befunde. *Arch. Zellforsch*. 16:300–365.

Gilson, E.T., T. Laroche, and S.M. Gasser. 1993. Teloeres and the functional architecture of the nucleus. *Trends Cell Biol*. 3:128–134.

Gotta, M., T. Laroche, A. Formenton, L. Maillet, H. Scherthan, and S.M. Gasser. 1996. The clustering of telomeres and colocalization with Rap1, Sir3, and Sir4 proteins in wild-type *Saccharomyces cerevisiae*. *J. Cell Biol*. 134:1349–1363.

Grushcow, J.M., T.M. Holzen, K.J. Park, T. Weinert, M. Lichten, and D.K. Bishop. 1999. *Saccharomyces cerevisiae* checkpoint genes MEC1, RAD17 and RAD24 are required for normal meiotic recombination partner choice. *Genetics*. 153:607–620.

Hawley, R.S. 1988. Exchange and chromosomal segregation in eukaryotes. *In* Genetic Recombination. R. Kucherlapati and G.R. Smimth, editors. American Society of Microbiology, Washington, D.C. 497–527

Hayashi, A., H. Ogawa, K. Kohno, S.M. Gasser, and Y. Hiraoka. 1998. Meiotic behaviors of chromosomes and microtubules in budding yeast: relocalization of centromeres and telomeres during meiotic prophase. *Genes Cells*. 3:587–601.

Hiraoka, Y. 1998. Meiotic telomeres: a matchmaker for homologous chromosomes. *Genes Cells*. 3:405–413.

Ishikawa, F., and T. Naito. 1999. Why do we have linear chromosomes? A matter of Adam and Eve. *Mutat. Res*. 434:99–107.

Jin, Q.-W., E. Trelles-Sticken, H. Scherthan, and J. Loidl. 1998. Yeast nuclei display prominent centromere clustering that is reduced in nondividing cells and in meiotic prophase. *J. Cell Biol*. 141:21–29.

Kane, S.M., and R. Roth. 1974. Carbohydrate metabolism during ascospore development in yeast. *J. Bacteriol*. 118:8–14.

Klein, F., T. Laroche, M.E. Cardenas, J.F.-X. Hofmann, D. Schweizer, and S.M. Gasser. 1992. Localization of RAP1 and topoisomerase II in nuclei and meiotic chromosomes of yeast. *J. Cell Biol*. 117:935–948.

Laroche, T., S.G. Martin, M. Gotta, H.C. Gorham, F.E. Pryde, E.J. Louis, and S.M. Gasser. 1998. Mutation of yeast Ku genes disrupts the subnuclear organization of telomeres. *Curr. Biol*. 8:653–656.

Loidl, J. 1990. The initiation of meiotic chromosome pairing: the cytological view. *Genome*. 33:759–778.

Loidl, J., F. Klein, and H. Scherthan. 1994. Homologous pairing is reduced but not abolished in asynaptic mutants of yeast. *J. Cell Biol*. 125:1191–1200.

Loidl, J., F. Klein, and J. Engebrecht. 1998. Genetic and morphological approaches for the analysis of meiotic chromosomes in yeast. *In* Nuclear Structure and Function. M. Berrios, editor. Academic Press, Inc., San Diego, CA. 257–285.

Louis, E.J., E.S. Naumova, A. Lee, G. Naumov, and J. Haber. 1994. The chromosome end in yeast: its mosaic nature and influence on recombination dynamics. *Genetics*. 136:789–802.

Marschall, L.G., R.L. Jeng, J. Mulholland, and T. Stearns. 1996. Analysis of Tub4p, a yeast gamma-tubulin-like protein: implications for microtubule-organizing center function. *J. Cell Biol*. 134:443–454.

Moens, P.B., and M.L. Ashton. 1985. Synaptonemal complexes of normal and mutant yeast chromosomes (*Saccharomyces cerevisiae*). *Chromosoma*. 91:113–120.

Moens, P.B. 1974. Quantitative electron microscopy of chromosome organization at meiotic prophase. *Cold Spring Harbor Symp. Quant. Biol*. 38:99–107.

Moses, M.J. 1968. Synaptinemal complex. *Annu. Rev. Genet*. 2:363–412.

Nag, D., H. Scherthan, B. Rockmill, J. Bhargava, and G.S. Roeder. 1995. Heteroduplex DNA formation and homolog pairing in yeast meiotic mutants. *Genetics*. 141:75–86.

Naito, T., A. Matsuura, and F. Ishikawa. 1998. Circular chromosome formation in a fission yeast mutant defective in two ATM homologues. *Nat. Genet*. 20:203–206.

Nimmo, E.R., A.L. Pidoux, P.E. Perry, and R.C. Allshire. 1998. Defective meiosis in telomere-silencing mutants of *Schizosaccharomyces pombe*. *Nature*. 392:825–828.

Padmore, R., L. Cao, and N. Kleckner. 1991. Temporal comparison of recombination and synaptonemal complex formation during meiosis in *S. cerevisiae*. *Cell*. 66:1239–1256.

Rhoades, M.M. 1961. Meioses. *In* The Cell: Biochemistry, Physiology, and Morphology. Vol. 3. J. Brachet and A.E. Mirsky, editors. Academic Press, New York, NY. 1–75.

Rockmill, B., M. Sym, H. Scherthan, and G.S. Roeder. 1995. Two RecA homologs facilitate meiotic chromosome synapsis by establishing connections between homologous chromosomes. *Genes Dev*. 9:2684–2695.

Rockmill, B., and G.S. Roeder. 1998. Telomere-mediated chromosome pairing during meiosis in budding yeast. *Genes Dev*. 12:2574–2586.

Roeder, G.S. 1997. Meiotic chromosomes: it takes two to tango. *Genes Dev*. 11:2600–2621.

Rasmussen, S.W., and P.B. Holm. 1978. Human Meiosis II. Chromosome pairing and recombination nodules in human spermatocytes. *Carlsberg Res. Commun*. 43:275–327.

Roth, R., and H.O. Halvorson. 1969. Sporulation of yeast harvested during logarithmic growth. *J. Bacteriol*. 98:831–832.

Scherthan, H., J. Loidl, T. Schuster, and D. Schweizer. 1992. Meiotic chromosome condensation and pairing in *Saccharomyces cerevisiae* studied by chromosome painting. *Chromosoma*. 101:590–595.

Scherthan, H., S. Weich, H. Schwegler, M. Härle, C. Heyting, and T. Cremer. 1996. Centromere and telomere movements during early meiotic prophase of mouse and man are associated with the onset of chromosome pairing. *J. Cell Biol*. 134:1109–1125.

Scherthan, H. 1997. Chromosome behaviour in earliest meiotic prophase. *In* Chromosomes Today. Vol. 12. H. Gill, J.S. Parker, and M. Puertas, editors. Chapman and Hall, London, UK. 217–248.

Shore, D. 1998. Telomeres–unsticky ends. *Science*. 281:1818–1819.

Strambio-de-Castillia, C., G. Blobel, and M.P. Rout. 1999. Proteins connecting the nuclear pore complex with the nuclear interior. *J. Cell Biol*. 144:839–855.

Sym, M., J.A. Engebrecht, and G.S. Roeder. 1993. ZIP1 is a synaptonemal complex protein required for meiotic chromosome synapsis. *Cell*. 72:365–378.

Sym, M., and G.S. Roeder. 1995. Zip1-induced changes in synaptonemal complex structure and polycomplex assembly. *J. Cell Biol*. 128:455–466.

Therman, E., and G.E. Sarto. 1977. Premeiotic and early meiotic stages in the pollen mother cells of eremus and in human embrionic oocytes. *Hum. Genet*. 35:137–151.

Thierry, A., L. Gaillon, F. Galibert, and B. Dujon. 1995. Construction of a complete genomic library of *Saccharomyces cerevisiae* and physical mapping of chromosome *XI* at 3.7 kb resolution. *Yeast*. 11:121–135.

Trelles-Sticken, E., J. Loidl, and H. Scherthan. 1999. Bouquet formation in budding yeast: initiation of recombination is not required for meiotic telomere clustering. *J. Cell Sci*. 112:651–658.

von Wettstein, D., S.W. Rasmussen, and P.B. Holm. 1984. The synaptonemal complex in genetic segregation. *Annu. Rev. Genet*. 18:331–413.

Wach, A., A. Brachat, R. Pohlmann, and P. Philippsen. 1994. New heterologous modules for classical or PCR-based gene disruptions in *Saccharomyces cerevisiae*. *Yeast*. 10:1793–1808.

Weiner, B.M., and N. Kleckner. 1994. Chromosome pairing via multiple interstitial interactions before and during meiosis in yeast. *Cell*. 77:977–991.

Yamamoto, A., R.R. West, J.R. McIntosh, and Y. Hiraoka. 1999. A cytoplasmic dynein heavy chain is required for oscillatory nuclear movement of meiotic prophase and efficient meiotic recombination in fission yeast. *J. Cell Biol*. 145:1233–1249.

Zakian, V.A. 1995. *Saccharomyces* telomeres: function, structure and replication. *In* Telomeres. E.H. Blackburn and C.W. Greider, editors. Cold Spring Harbor Laboratory Press, Cold Spring Harbor, NY. 107–138.

Zickler, D., and L.W. Olson. 1975. The synaptonemal complex and the spindle plaque during meiosis in yeast. *Chromosoma*. 50:1–23.

Zickler, D., and N. Kleckner. 1998. The leptotene-zygotene transition of meiosis. *Annu. Rev. Genet*. 32:619–697.